Inorganic Chemistry

Article

pubs.acs.org/IC

Slow Magnetic Relaxations in Manganese(III) Tetra(*meta*-fluorophenyl)-porphyrin-tetracyanoethenide. Comparison with the Relative Single Chain Magnet *ortho* Compound

Z. Tomkowicz,*[,†] M. Rams,[†] M. Bałanda,[‡] S. Foro,[§] H. Nojiri,[∥] Y. Krupskaya,[⊥] V. Kataev,[⊥] B. Büchner,[⊥] S. K. Nayak,[#,¶] J. V. Yakhmi,[×] and W. Haase*[,#]

[†]Institute of Physics, Jagiellonian University, Reymonta 4, 30-059 Kraków, Poland

[‡]H. Niewodniczański Institute of Nuclear Physics PAN, Radzikowskiego 152, 31-342 Kraków, Poland

[§]Clemens-Schöpf-Institut für Organische Chemie und Biochemie, Technische Universität Darmstadt, Petersenstrasse 22, D-64287 Darmstadt, Germany

[∥]Institute for Materials Research, Tohoku University, Katahira 2-1-1, Sendai 980-8577, Japan

[⊥]Institute for Solid State Physics, IFW Dresden, Helmholtzstrasse 20, D-01069 Dresden, Germany

[#]Eduard-Zintl-Institut für Anorganische und Physikalische Chemie, Technische Universität Darmstadt, Petersenstrasse 20, D-64287 Darmstadt, Germany

[×]Technical Physics & Prototype Engineering Division, Bhabha Atomic Research Centre, Mumbai -400 085, India

Supporting Information

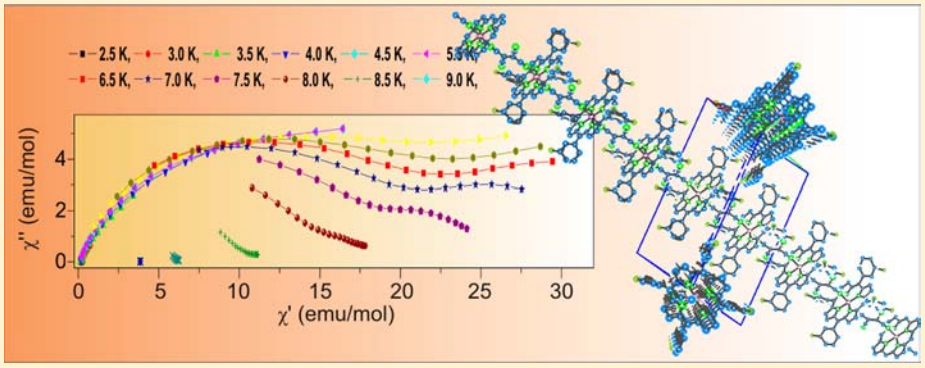

ABSTRACT: Mn(III) tetra(*meta*-fluorophenyl)porphyrin-tetracyanoethenide coordination polymer (abbreviated *meta*-F) was synthesized and crystallographically and magnetically characterized. The compound crystallizes in the space group *C*2/*c* with four equivalent molecules in the unit cell arranged along two symmetry related nonparallel linear chain directions. Magnetic properties were studied by SQUID dc magnetization and ac susceptibility techniques and high field-high frequency electron spin resonance (HF-ESR). Glassy transition to a ferromagnetic-like state is observed at 10 K accompanied by slow magnetic relaxations. The glassiness is interpreted as due to 3D domain wall pinning. In a bias dc magnetic field the width of the relaxation time distribution decreases and the relaxations become similar to the relaxations of the single chain magnet Mn(III) tetra(*ortho*-fluorophenyl)porphyrin-tetracyanoethenide (abbreviated *ortho*-F), for which comparative HF-ESR studies were also conducted in this work. Magnetic properties of these two compounds are compared, and the nature of magnetic relaxations in *meta*-F is discussed.

1. INTRODUCTION

It is well-known that 1-dimensional systems do not display long-range magnetic order. Nevertheless, ferro- or ferrimagnetic chains comprising in their structure highly anisotropic ions of transition elements are of great interest due to slow magnetic relaxations. These systems, known as single chain magnets (SCM), are intensively investigated since 2001.[1]

One of the rich families of 1-dimensional magnetic systems are coordination polymers composed of Mn porphyrin−radical molecule pairs. Plenty of such compounds may be obtained by various substitutions, and their magnetic properties may be tuned in a broad range, as shown by Miller et al., who synthesized many compounds of this family and characterized them structurally and magnetically.[2−5] Haase et al. synthesized Mn-porphyrin−TCNE compounds (TCNE-tetracyanoethenide) with long alkoxy chains attached at the porphyrin ring periphery at the *para* position of the phenyl ring, see Figure 1.

Received: July 10, 2012
Published: September 5, 2012

dx.doi.org/10.1021/ic3014927 | *Inorg. Chem.* 2012, 51, 9983−9994

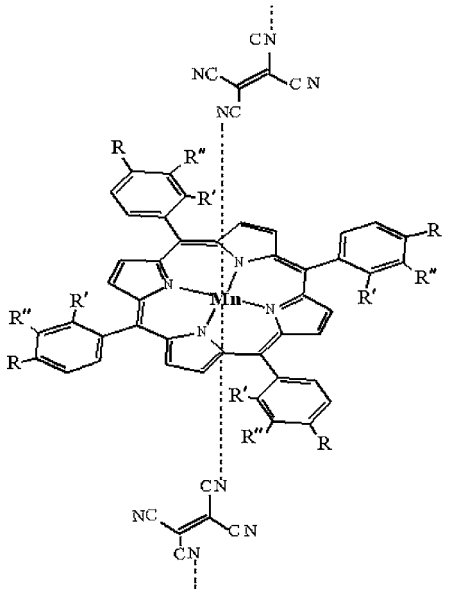

Figure 1. Molecular structure of Mn(III) tetra(fluorophenyl)-porphyrin-tetracyanoethenide. R, R′, R″ labels denote *para*, *ortho* and *meta* positions of the phenyl ring, respectively.

For these compounds interesting magnetic properties were reported at low temperatures[6,7] and even liquid crystalline properties[8] above room temperature. In spite of the long interchain distance ~30 Å, a transition into magnetically ordered state was observed at about 10−20 K for all these substitutions. In the course of further studies special attention was paid to the fluorine atom attached at different positions of the phenyl ring. It was interesting to see how the strongly electronegative fluorine ion influences magnetic exchange and anisotropy of Mn(III) ion. Compounds with *para* and *ortho* substitutions of F were studied also by Miller and co-workers. They reported that *para*-F compound exhibits a magnetic phase transition at T_c = 28 K and that the intrachain value of exchange integral J for this compound is large, above 300 K.[4] (J is defined by the Hamiltonian $\mathcal{H} = -J\, S_i \cdot S_j$.) For *ortho*-F an anomaly of ac magnetic susceptibility at 12.5 K was observed and interpreted as antiferromagnetic transition.[5] Consistent results for *para*-F compound were obtained by Balanda et al.[7], but as for the *ortho*-F substitution, the antiferromagnetic transition was not confirmed by these researchers. Instead, the compound was reported to be a SCM.[9] The character of magnetic relaxations in *ortho*-F was investigated, and it was shown that they have the soliton character.[10] In continuation of these studies the fluorine atom was substituted at the *meta* position. As we will show in this report, the compound obtained shows 3D glassy transition at T_c = 10 K, which is typical for this family of compounds. The nature of the glassiness observed may be connected with the 3D- domain wall pinning[11] or with growing of fractal clusters as proposed by Etzkorn et al.[12] Slow relaxations were observed near transition and down to the lowest temperature attainable (1.8 K). With increasing applied dc magnetic field these relaxations became similar to those observed for the *ortho*-F compound. Quite recently a paper of Pini et al. has appeared[13] (see also ref 14) describing the effects of an applied magnetic field and finite size of chains for SCM. Their $\chi_{ac}(T)$ curves have two maxima: the low temperature one is frequency dependent, and the high temperature one is not. This behavior, although similar at first sight, just differs in the last point from the behavior observed in the present work. It should be noted that slow relaxations below critical temperature T_c were confirmed by reports of SCM-like behavior in an ordered magnetic phase of compounds consisting of antiferromagnetically coupled chains of Mn(III)$_2$−Ni(II)[15] or Mn(III)−Ni(II) units[16] as well as of ferromagnetically coupled chains of Co(II)−radical units.[11,17]

The question arises about the character of relaxations observed in this work. As known, spin dynamics of quasi-1D magnetic systems above T_c is governed in general by spin solitons, breathers and spin waves. Solitons are bound states of spin waves, which may have energy lying below the spin wave band.[18] But in contradistinction to spin waves, they are localized excitations, which can freely move in the crystal lattice. Below T_c a weak interchain coupling leads to a 3D ordered structure with static domains. Nonetheless, narrow solitons, called kinks, were experimentally observed both above and below phase transition temperature in quasi-1D systems.[19] It was also theoretically shown that, for weakly coupled chains, static solitons may occur in the ordered phase, ordering of which is induced by pairing of solitons belonging to the same chain.[20] Morgunov et al.[21] observed spin soliton and standing spin wave resonances, which simultaneously appeared in ESR spectra of some chiral 2D and 3D molecular crystals in their ferromagnetic state. A powerful method, which allows direct study of a broad spectrum of magnetic excitations, is the high field, high frequency ESR (HF-ESR). We included HF-ESR spectroscopy for investigations of our Mn porphyrin-TCNE compounds. We were interested to compare excitation gaps for *meta*- and *ortho*-F compounds, the values of which should reflect difference in electronic parameters and a character of magnetic excitations. It is worth noting that HF-ESR was already used to study a Mn(III) porphyrin complex MnTPPCl (Mn axially ligated by one Cl ligand).[22] As a result of this study the anisotropy gap Δ was determined to be 6.9 cm^{-1}, which gives the value of the single ion zero field parameter $D = -\Delta/3 = -2.29$ cm^{-1} (−3.3 K).

The crystallographic and magnetic characterization of the *meta*-F compound, HF-ESR investigations of both *meta*- and *ortho*-F compounds and their comparative study is the aim of this work. We hope to shed light on the problem of coexistence of phase transition and slow relaxations in quasi-1D systems.

2. EXPERIMENTAL SECTION

2.1. Synthesis of Manganese(III) tetrakis(3-fluorophenyl)-porphyrin-tetracyanoethenide (Scheme 1). *2.1.1. Synthesis of* ***1****.*[23] Freshly distilled pyrrole (13.42 g, 0.2 mol) and 3-fluorobenzaldehyde (24.82 g, 0.2 mol) were added dropwise simultaneously to a boiling propionic acid (750 mL). Refluxing was continued for 30 min, and the mixture was allowed to stand overnight at ambient temperature. The dark solution was filtered, and the solid was washed with methanol and water and dried. The crude solid was purified by column chromatography (silica, eluant CH_2Cl_2−hexane = 8:2) to get pure tetrakis(3-fluorophenyl) porphyrin (**1**) as a purple powder (5.5 g, 16%). ^{1}H NMR ($CDCl_3$): δ 8.92 (s, 8H, pyrrole β-H), 8.04 (m, 8H), 7.72 (m, 4H), 7.53 (m, 4H), −2.82 (bs, 2H). IR (film): 3434, 1644, 1612, 1215, 757 cm^{-1}.

2.1.2. Synthesis of ***2****.*[24] A solution of **1** (2.75 g, 4 mmol) and Mn$(OAc)_2 \cdot 4H_2O$ (9.8 g, 40 mmol) in dry *N*,*N*-dimethylformamide (30 mL) was refluxed under argon (4 h) when thin layer chromatography (TLC) showed complete consumption of **1**. The mixture was cooled to ambient temperature and poured into 1400 mL of ice-cooled brine solution when a solid precipitated. The solid was filtered, washed with distilled water (1500 mL) and dried. The green solid was dissolved in a minimum amount of methanol (350 mL), and the solution was poured

dx.doi.org/10.1021/ic3014927 | Inorg. Chem. 2012, 51, 9983−9994

Scheme 1

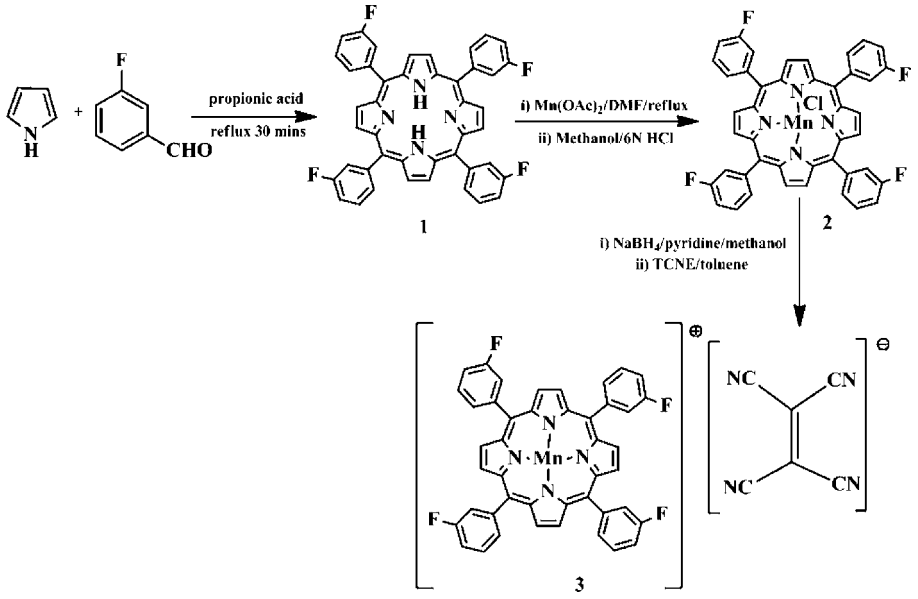

into aqueous 6 N HCl (350 mL). The solution was allowed to stand overnight, filtered, washed with water and dried in air. The brown colored solid was crystallized from a toluene−hexane mixture to afford pure tetrakis(3-fluorophenyl)porphyrin manganese(III) chloride (**2**) as a green crystalline solid (2.10 g, 68%).

2.1.3. Synthesis of ***3****.*[25] Using a Schlenck apparatus the compound **2** (1.55 g, 2 mmol) was dissolved in dry methanol and dry pyridine, and to that $NaBH_4$ was added. The mixture was then refluxed (30 min) and cooled to ambient temperature, argon purged methanol was added and the mixture was kept standing overnight. The mixture was filtered under inert atmosphere, washed with dry methanol and finally dried under vacuum to get a pink colored solid. The solid was dissolved in argon purged toluene, and a solution of tetracyanoethylene (0.512 g, 4 mmol) in argon purged toluene was added to it. The mixture was briefly stirred and kept standing for 4 days under argon without stirring. The precipitated dark solid was washed with argon purged toluene and dried under vacuum for 2 h to get a dark pink solid (0.560 g, 32%). IR (Nujol): 2198 (m), 2156 cm^{-1}.

Two kinds of material were obtained from synthesis: finely dispersed polycrystalline material and small crystallites. The crystallites were very brittle and broke down under a slight touch. For these studies mainly powdered crystallites were used.

2.2. Methods of Investigation. *2.2.1. Crystal Structure.* The crystal structure was determined from X-ray data collection ($2\Theta_{max}$ = 52.74°) on an Oxford Xcalibur diffractometer. The lattice parameters were refined by 5830 reflections (Θ = 2.59−22.34°). The structure was solved by the direct method using SHELXS-97, and refinement was done with SHELXL-97. The H atoms were positioned with idealized geometry using a riding model with C−H = 0.93 Å, and U_{iso}(H) values were set equal to 1.2U_{eq}(parent atom).

2.2.2. Magnetic Ac and Dc Measurements. These measurements were performed with a Quantum Design SQUID magnetometer, model MPMS-XL5. The sample for measurements was powdered and pressed into a pellet in order to avoid the reorientation of grains in the external magnetic field. The data were corrected for the diamagnetic contribution as deduced with the use of a table of Pascal constants. One good shaped crystallite was chosen for magnetization measurements and secured in melted eicosane.

2.2.3. High-Field/High-Frequency Electron Spin Resonance (HF-ESR). These measurements were performed in the transmission Faraday geometry for two compounds, *meta*-F and *ortho*-F, for comparison. Measurements were done on loose powder samples. The small powder particles were self-oriented in the magnetic field during the measurements.

The *meta*-F compound was studied in Dresden. The measurements were done in a frequency range 332−528 GHz in static magnetic fields up to 15 T using a homemade spectrometer based on a Millimeter-wave Vector Network Analyzer (AB Millimetré).[26]

The *ortho*-F compound was studied in Sendai. The experimental setup is described in ref 27. Measurements were performed in pulse magnetic fields. The time of the pulse was ∼10 ms.

3. CRYSTAL STRUCTURE DESCRIPTION

The crystal structure of the studied *meta*-F compound is shown in Figure 2; see also CIF file in Supporting Information. In Table 1 the crystallographic parameters are given. This structure belongs to the monoclinic space group *C*2/*c* with four crystallographically equivalent pairs of the porphyrin and TCNE molecules in the elementary crystal cell. These porphyrin-TCNE units are alternatively ordered along two symmetry related chains running parallel to diagonals of the *a*,*b* crystal cell wall. Thus, the angle between Mn−Mn bonds of two chains, as being equal to the angle between diagonals, equals 66°. It should be noted that the porphyrin planes are not exactly perpendicular to the Mn−Mn direction: the declination angle is 6.05°. Manganese atoms are located in the inversion center in a distorted octahedral coordination by 2N1 and 2N2 nitrogen atoms in the porphyrin plane and 2N3 atoms perpendicular to the plane. Because of the elongated Mn−N3 distance, the N3−Mn−N3 direction is expected to be the magnetic easy direction. The angle between the linear N3−Mn−N3 bonds of two chains is 53.9°. The two symmetry independent phenyl rings show statistical disorder. One phenyl ring is statistically distributed between two equilibrium orientations differing by 180°, and the second phenyl ring is disordered, as is well characterized via the high thermal parameters of some carbon atoms.

Two chain directions is the most distinguishing feature of the *meta*-F crystal structure. The *ortho*-F compound, as other compounds of this family, has only one chain direction. Also the character of disorder in *ortho*-F differs from that in *meta*-F. For the *ortho* compound the $[TCNE]^{\bullet-}$ molecule is orientationally disordered with the minor form (20.5%) being rotated by 90° (in the same plane) with respect to the major form (79.5%). Besides, F in *ortho-F* is disordered over two sites on both sides of the phenyl ring in a similar proportion.[28]

dx.doi.org/10.1021/ic3014927 | *Inorg. Chem.* 2012, 51, 9983−9994

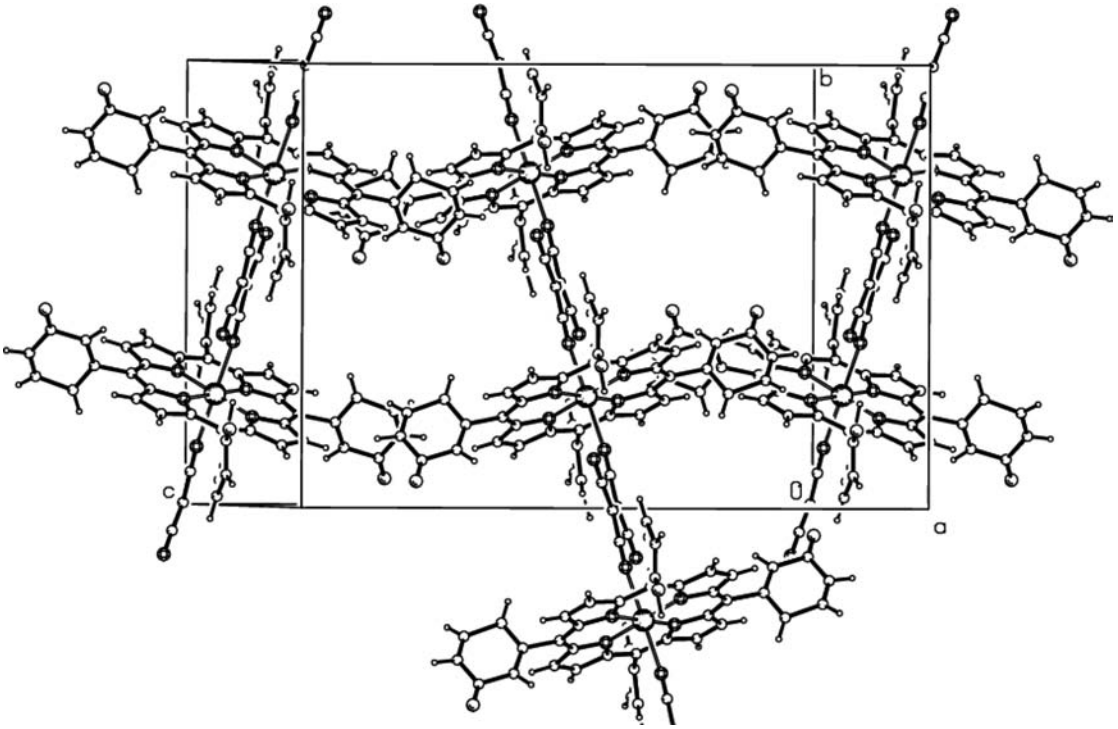

Figure 2. Crystallographic structure of Mn(III) tetra(*meta*-fluorophenyl)porphyrin-tetracyanoethenide. The chain in the middle is inclined to the plane of the drawing in the opposite direction than the side chains.

Table 1. Crystallographic Parameters of Mn(III) Tetra(*meta*-fluorophenyl)porphyrin-tetracyanoethenide

molecular formula	$C_{60}H_{24}F_4MnN_8$
formula weight	987.81
temp (K)	299(2)
crystal system	monoclinic
space group	*C*2/*c*
a (Å)	11.3331(7)
b (Å)	17.4406(9)
c (Å)	25.1790(10)
α (deg)	90.00
β (deg)	102.710(4)
γ (deg)	90.00
vol (Å^3)	4854.8(4)
Z	4
density (calcd) (Mg/m^3)	1.351
abs coeff (mm^{-1})	0.337
F(000)	2004
crystal size (mm^3)	0.46 × 0.30 × 0.26
theta range for data collection (deg)	4.13 to 26.37
h k l ranges	−14, 7, −21, 21, −31, 31
reflns collected	24219
indep reflns	4935 [*R*(int) = 0.0653]
abs corr	semiempirical from equivalents
max and min transm	0.9175 and 0.8605
data/restraints/params	4935/15/403
goodness-of-fit on F^2	1.092
final *R* indices [*I* > 2sigma(*I*)]	R1 = 0.0782, wR2 = 0.2160
R indices (all data)	R1 = 0.1002, wR2 = 0.2347
largest diff peak and hole (e Å^{-3})	0.543 and −0.354

Another structural difference between *meta*-F and *ortho*-F is a considerable anisotropy in the porphyrin plane for *meta*-F as can be seen from the comparison of Mn−N1 and Mn−N2 distances (Table 2).

Table 2. Selected Interatomic Distances (Å) and Bond Angles (deg) in *meta*-F and *ortho*-F Compounds

distance or bond angle	*meta*-F	*ortho*-F[5]
Mn−N1 in plane	2.08	2.000
Mn−N2 in plane	2.013	2.016
Mn−N3 out of plane	2.327	(2.309; 2.33) 2.313[a]
Mn−Mn along chains	10.400	10.185
Mn−Mn between chains	14.900	11.081
Mn−F	8.07	5.32
N1−Mn−N3	90.40; 89.60	92.9; 87.1
N1−Mn−N2	90.03; 89.97	90.55; 89.45
C23−C24−C24′	119.78	117.3; 117.3
N3−C23−C24	178.75	(179.6; 173) 178.8[a]
Mn−N3−C23	172.10	(150.3; 140) 148.6[a]
MnN_4−[TCNE][b]	76.3	(55.6; 53.9) 55.4[a]

[a]Three values for *ortho*-F are for the major, minor and the occupancy weighted average, respectively.[5] [b]Dihedral angle between mean planes. Numeration of atoms is according to CIF file in Supporting Information.

4. MAGNETIC STUDIES

4.1. Static Properties. In Figure 3 the temperature dependence of dc magnetic susceptibility is presented in the form of the effective magnetic moment defined as $\mu_{eff} = (8\chi_{mol}T)^{1/2}$. The measurement was done in a magnetic field of 1000 Oe. Ac susceptibility data measured at the frequency of 1 Hz and the amplitude of the driving magnetic field of 3 Oe (see the next section) are also shown for comparison. The high maximum of ac data is seen at the temperature of 7.5 K, a little lower than the position of dc maximum 8.0 K. At higher temperatures $\mu_{eff}(T)$ dependence shows a minimum, as expected for a ferrimagnetic chain. This minimum (shallow, not seen in the scale of the figure) falls at the temperature ∼130 K, much lower than observed for the *ortho*-F compound, for which it falls at about

dx.doi.org/10.1021/ic3014927 | *Inorg. Chem.* 2012, 51, 9983−9994

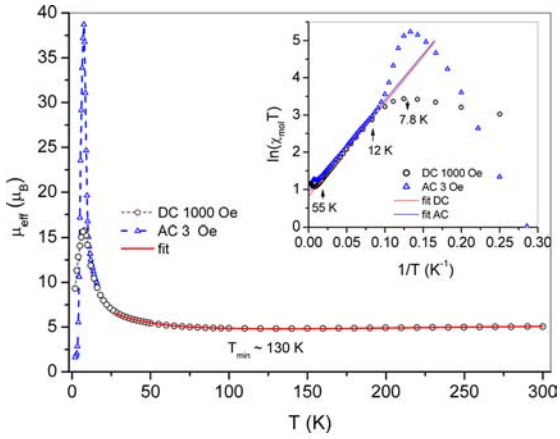

Figure 3. Temperature dependence of $\mu_{eff} = (8\chi_{mol}T)^{1/2}$ for *meta*-F obtained in static magnetic field of 1000 Oe (open circles). Ac data are shown for comparison (open triangles connected by the dashed line). Inset: the same data presented as $\ln(\chi_{mol}T)$ vs reciprocal temperature. Solid lines are fits (see the text).

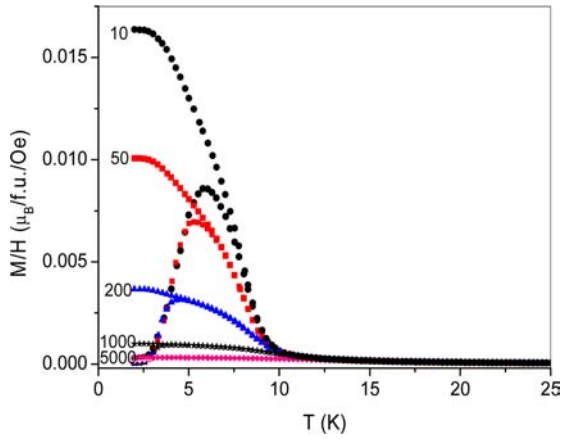

Figure 4. Field cooling (monotonous dependences) and zero field cooling magnetization (curves with maximum) plotted as a function of temperature for *meta*-F in various static magnetic fields, strengths of which are given in oersteds.

room temperature. In order to determine the exchange integral J, the Seiden model[29] was used, which is based on the isotropic Hamiltonian,

$$\mathcal{H} = -J\sum_{i=1}^{N-1}[\vec{S}_{Mn,i} + \vec{S}_{Mn,i+1}]\vec{s}_{TCNE,i} \quad (1)$$

where $S_{Mn,i} = 2$ is the spin of Mn(III) ion and $s_{TCNE,i} = 1/2$ is the spin of the tetracyanoethenide radical.

By fitting the data in the temperature range 30−300 K the value of J equal to -100 ± 8 K was obtained in comparison with the value −217 K for the *ortho*-F compound. This considerable difference is consistent with the greater value of the bonding Mn−N−C angle and dihedral MnN_4−[TCNE] angle between mean planes for the *meta*-F compound (see the last two lines in Table 2), according to magnetostructural correlations established by Miller et al. for this family of compounds.[30] In the inset to Figure 3 the same data are presented in another form $\ln(\chi_{mol}\cdot T)$ vs reciprocal temperature. The influence of the applied magnetic field is seen below 10 K. The linear part, observed in some temperature range, is in accord with the anisotropic Heisenberg model, which predicts the following relation:

$$\chi_{\parallel}T \propto e^{\Delta_\xi/kT} \quad (2)$$

valid for the parallel susceptibility, which, however, is dominant in this model. Δ_ξ is the creation energy of a domain wall in the chain.[31] The value of Δ_ξ, obtained from the linear fit, is equal to 25 ± 2 K in comparison with the value of 60 K obtained for *ortho*-F.

Figure 4 presents field cooling (FC) and zero field cooling (ZFC) magnetization data (normalized to the susceptibility) plotted as a function of temperature. At 10 K a sharp upraise of M/H is seen by decreasing temperature, which is the manifestation of a phase transition, and a bifurcation point appears at some lower temperature for every value of the superimposed dc magnetic field. The bifurcation point moves to lower temperature with increasing strength of the magnetic field. The falling low temperature part of the ZFC curve is common for all fields (compare χ'' behavior, Figure 9b). By the change of field from 50 up to 5000 Oe the bifurcation point for *meta*-F shifts from 5.8 to 3.0 K. For *ortho*-F by the same field change this shift is much smaller: from 4.8 to 4.0 K.[9]

As seen, there are some differences in FC vs ZFC behavior for *meta*-F in comparison with *ortho*-F. There exists the common point of the divergence of all curves for various fields at 10 K. For small fields ZFC curves are not falling sharply down below the bifurcation point but they deviate still going up with decreasing temperature. This diverse FC vs ZFC behavior may be interpreted as domain wall pinning or by the presence of strongly interacting spin clusters.[32]

In Figure 5 ZFC magnetic hysteresis loops are shown, which were recorded at 1.8 K. One of the loops (smaller) is for the

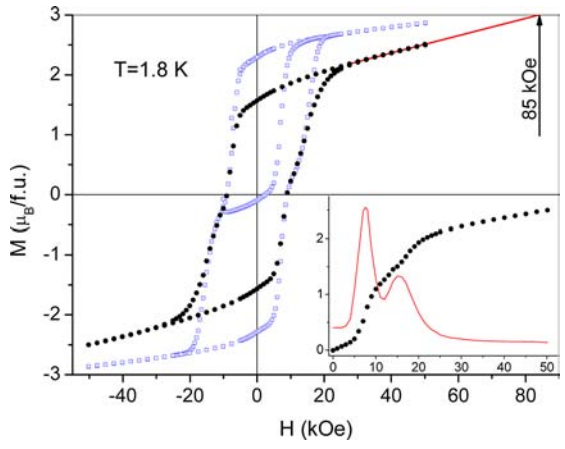

Figure 5. ZFC magnetic hysteresis loops of *meta*-F recorded at 1.8 K. The smaller loop is for polycrystalline sample. The red line is extrapolation to intersection with the ordinate of 3 μ_B. The greater loop is for a crystallite oriented to obtain the maximum value of the highest field magnetization. For the crystallite the minor loop was measured instead of the virgin curve. In the inset the virgin magnetization curve is shown together with its derivative.

polycrystalline material, the second one (greater) for a crystallite. The orientation of the crystallite was chosen to obtain a maximum value of magnetization at the highest magnetic field. As seen, the coercive field is 9.0 kOe, more than two times lower than observed for the *ortho*-F compound. No saturation is observed at 50 kOe, even for the crystallite at the chosen

dx.doi.org/10.1021/ic3014927 | Inorg. Chem. 2012, 51, 9983−9994

orientation. The virgin magnetization curve is shown in the inset to Figure 5 together with its derivative. Two peaks of the derivative are seen: one at 7.5 kOe and the second at 15 kOe. The relation of fields, being 1:2 at 1.8 K changes with increasing temperature. This two-step magnetization curve seems to be related to the presence of two families of chains in the *meta*-F compound. The lower field reverses one family and then a higher external field is required to reverse the second family, because the external field is partially compensated by molecular field.

The extrapolation of the high field magnetization of the polycrystalline sample to its expected saturation value[33] $g\mu_B S_T$ gives the anisotropy field H_a= 85 kOe, at g = 2.0 and S_T = 3/2 (Figure 5). This H_a value gives the estimation of the anisotropy energy per molecule,

$$K_A = \frac{1}{2}(g_{Mn}S_{Mn} - g_{TCNE}s_{TCNE})\mu_B H_a \quad (3)$$

equal to 8.5 K. By formally equating $K_A = DS_{Mn}^2$ the zero field splitting parameter of the single Mn(III) ion $|D|$ = 2.1 K is obtained. It should be noted that eq 3 was used for the case of two directions of anisotropy, which, however, for a powder sample at saturation should be correct. For *ortho*-F the analogous procedure gives H_a = 117.6 kOe, thus K_A= 11.8 K and $|D|$ =2.95 K.[9]

4.2. Dynamic Properties. *4.2.1. Dc Measurements.* Magnetization, when observed in a long time scale, is not the static property. In Figure 6 the time dependence of thermo-

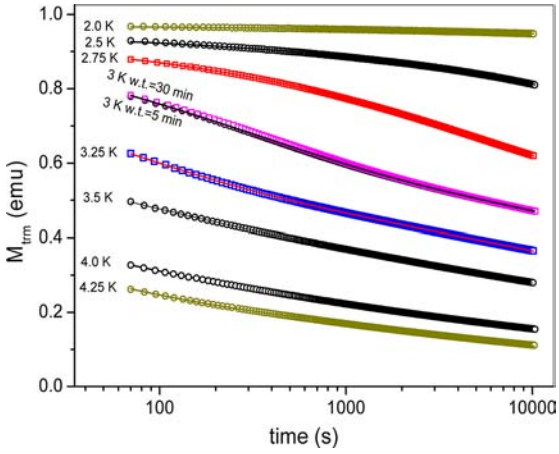

Figure 6. Thermoremanent magnetization of *meta*-F measured as a function of time at various temperatures. The time dependence at 3 K was measured with the waiting time 5 and 30 min. Solid lines are fits, see text. The values of M have no relation to those in Figure 7 because a new sample weight was used.

remanent magnetization is plotted vs logarithm of time. In this experiment the sample was first magnetized in field of 50 kOe, then the field was off and the magnetization was measured as a function of time at various temperatures. The curves in Figure 6 look differently than the analogous data for the *ortho*-F compound.[9] The data for the *meta*-F compound can be fitted using the following relation:

$$M_{trm} = \sigma_0 + M_0 e^{-(t/\tau)^{1-n}} + a \ln t \quad (4)$$

where $n \approx 0.5$, $a \approx -0.04$.

The above relation contains many fitting parameters (σ_0, M_0, n, τ, a), but the additional a·ln (t) term is necessary to obtain a good fit. The presence of this term means constant in time and homogeneous activation energy distribution. The factor a has meaning of magnetic viscosity, which is a spin glass property. Here, the glassiness may originate from the domain wall pinning.[34] There is no waiting time dependence (as checked for 5 and 30 min, see the curve at 3 K), being a characteristic property of spin glasses.[35]

Let us see now how the superimposed dc field influences the time dependences. In this experiment the field was not completely off. The corresponding plots obtained in the bias field of 1000 Oe are shown in Figure 7. All these dependences can be nicely fit with eq 4 without the ln(t) term.

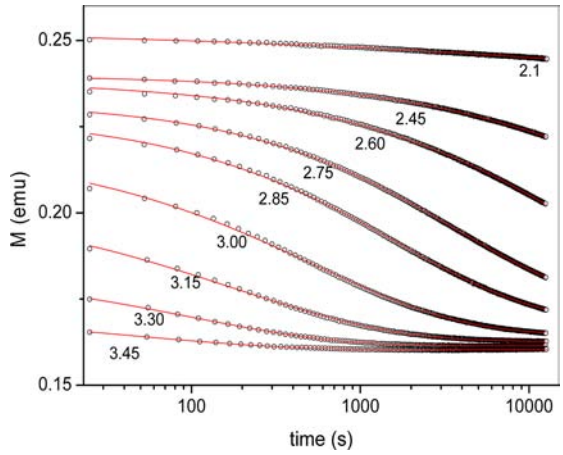

Figure 7. Magnetization of *meta*-F as a function of time measured at various temperatures and in the superimposed dc magnetic field of 1000 Oe. Measurement started after switching the field from 50 to 1 kOe. Solid lines are fits, see text.

From these fits the average relaxation time τ was obtained. Reciprocal temperature dependence of ln τ is shown in Figure 13 together with the corresponding ac data. From the slope of this plot the activation energy E_a can be determined according to the Arrhenius equation:

$$\tau = \tau_0 e^{E_a/kT} \quad (5)$$

The fitted parameters are E_a = 64 ± 5 K and $\tau_0 = (1.9 \pm 0.6) \times 10^{-8}$ s.

4.2.2. Ac measurements. Figure 8a presents temperature dependence of the ac susceptibility of *meta*-F, measured for various frequencies with no superimposed dc magnetic field. Here, it is seen that both χ' and χ'' maxima move to higher temperature with increasing frequency and, while the maximum value of the χ' component decreases with increasing frequency, the maximum value of χ'' remains almost constant. When dc magnetic field is superimposed, both ac susceptibility components are quickly suppressed, which is shown in Figure 8b for the constant frequency of 10 Hz.

How frequency characteristics change in a superimposed dc magnetic field is separately shown in Figure 9. As is seen, these characteristics differ remarkably from those obtained in zero dc magnetic field. It looks like as if both χ' and χ'' were composed of two constituents. The first one, with its χ' maximum near 8.5 K in small field, is weakly (or not) dependent on frequency. It slightly moves with increasing dc field to higher temperatures (9.0 K in 1000 Oe) and being strongly suppressed in a field of 1000 Oe is expected to disappear with further field increasing, see Figure 9c (its χ'' companion disappeared earlier). The

dx.doi.org/10.1021/ic3014927 | Inorg. Chem. 2012, 51, 9983−9994

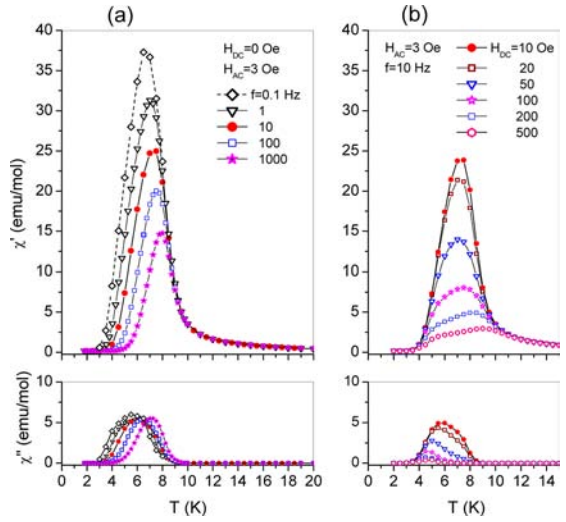

Figure 8. Temperature dependence of both components χ' and χ'' of the ac magnetic susceptibility of *meta*-F compound measured for various frequencies at zero static magnetic field (a) and for various static superimposed magnetic fields at the constant frequency of 10 Hz (b). The amplitude of the driving magnetic field H_{ac} is 3 Oe.

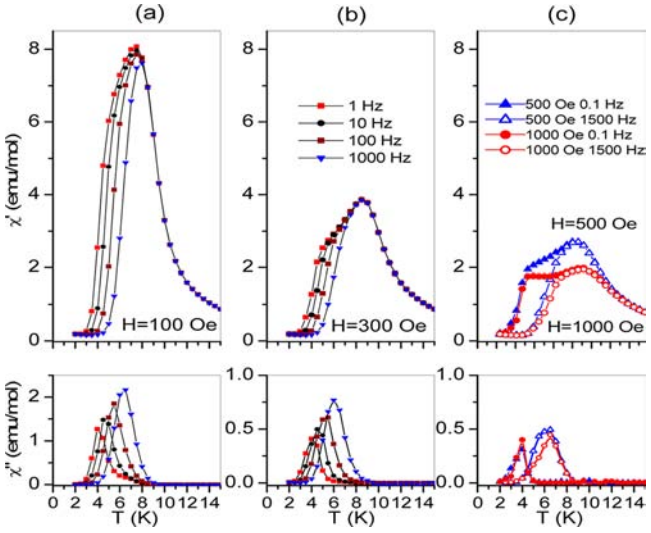

Figure 9. Temperature dependence of both components χ' and χ'' of the ac magnetic susceptibility of *meta*-F compound measured for various frequencies at four static magnetic fields, 100 Oe (a), 300 Oe (b), 500 and 1000 Oe (c). Note, that panels a and b have the same legend. The amplitude of the driving magnetic field H_{ac} is 3 Oe.

frequency dependence is associated mainly with the second constituent, which separates from the first χ' constituent moving together with the accompanying frequency dependent χ'' constituent to lower temperatures. It can be seen that this χ'' constituent (at least in fields below 500 Oe) increases with increasing frequency, which is at variance with the case of zero dc field.

It is worth noting that poorly crystallized powder samples (with grain size close to one-domain nanoparticles) from another synthesis batch show ac behavior in zero dc field, which is like ac behavior in nonzero field described above. It means their ac characteristics in zero field are like this in Figure 9b.[36]

It is also interesting to see relaxations in the frequency domain. Figure 10 presents frequency dependences of χ' and χ'' measured for various temperatures without (a) and with dc bias field (b). As seen in panel a there is a broad distribution (one can discern two distributions) of relaxation times, however, in

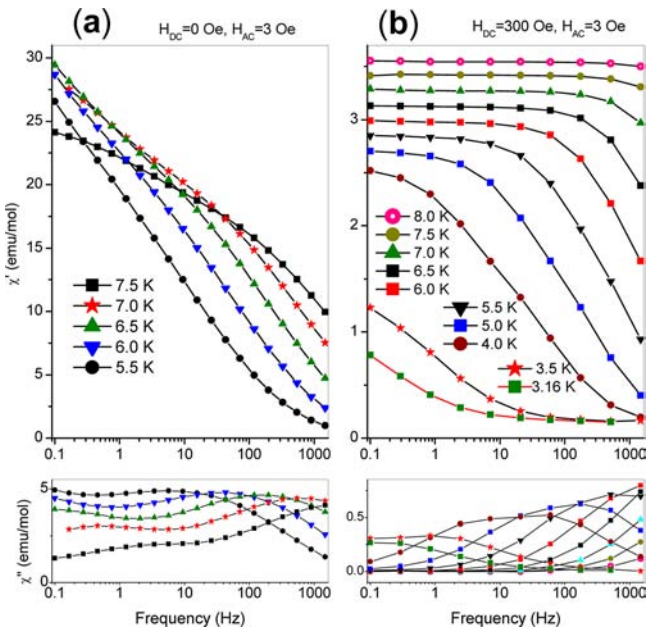

Figure 10. Frequency dependence of ac susceptibility for *meta*-F measured at various temperatures. (a) Data obtained in zero dc bias field. (b) Data obtained in dc bias field of 300 Oe. Solid lines are guides for eye.

the bias field of 300 Oe (see panel b) the distribution drastically narrows and relaxation has a Debye character.

Narrowing of the distribution of relaxation times in field can be also shown by means of Argand diagrams. In Figure 11

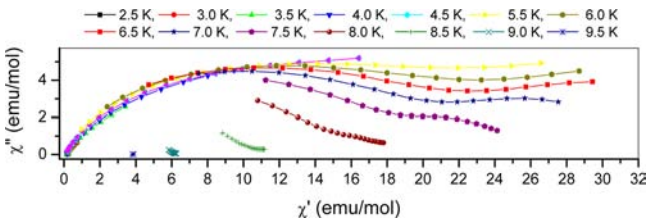

Figure 11. Argand plots for *meta*-F obtained at various temperatures with no superimposed dc magnetic field.

Argand diagrams for *meta*-F obtained with no superimposed magnetic field are shown for various temperatures. As is seen, the distribution of relaxation times is very broad. Again, two distributions can be differentiated, as is seen, e.g., for T = 7.5 K. The width of distribution can be characterized by the parameter α, obtained from fitting arcs of the $(1 - \alpha)\pi$ size to the χ'' vs χ' data. When dc magnetic field is applied, the distribution drastically narrows and only one distribution is present, as shown in Figure 12a for T = 5.5 K. In dc field of 1000 Oe α equals 0.24. The values of α obtained for *meta*-F can be compared with the α value for the *ortho*-F compound. The latter one equals 0.12, see Figure 12b, and is completely independent of temperature. The value of α expected for the ideal single chain magnet should be equal to zero (single relaxation time), but for the real single chain magnets such values as ~0.12 were reported in literature for powder samples.[37,38]

dx.doi.org/10.1021/ic3014927 | Inorg. Chem. 2012, 51, 9983−9994

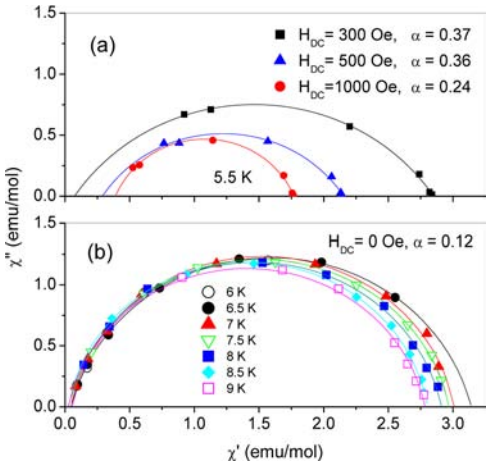

Figure 12. Comparison of Argand plots for *meta*-F compound obtained at 5.5 K in various dc magnetic fields (a) and for *ortho*-F obtained at various temperatures in 0 Oe dc field (b). The arcs are fits to the data.

Using the data shown above, temperature dependence of the relaxation time can be determined. Taking the temperature for the maximum of $\chi''(T)_{f,H}$ curves measured by fixed f and bias field H and assuming that the relaxation time at the temperature of maximum is equal to $1/(2\pi f)$, the diagram presenting $\ln(\tau)$ vs reciprocal temperature can be constructed. In Figure 13 four linear dependences obtained from ac high

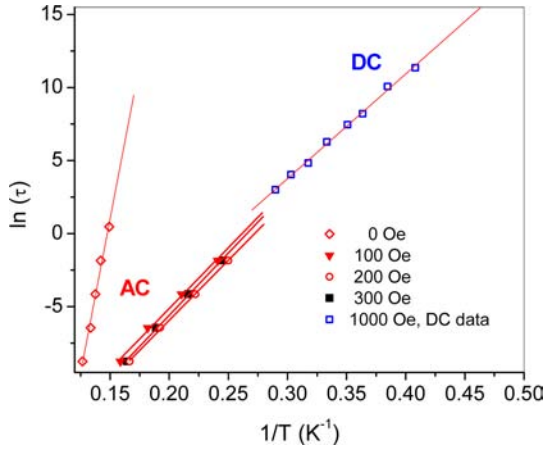

Figure 13. Natural logarithm of the relaxation time vs reciprocal temperature dependence for *meta*-F compound. The high temperature data (red color) were obtained from ac susceptibility measurements. The left (most steep) line was obtained in zero bias magnetic field, and the other three lines were obtained for nonzero bias magnetic fields. Dc data are also shown (see section 4.2.1). Solid lines are fits.

temperature data (above 4 K) are shown and compared with the low temperature dc SQUID data obtained below 3 K in dc field of 1000 Oe. One of the ac dependences refers to zero bias dc field, and the other ones refer to the case of the bias dc field equal to 100, 200, and 300 Oe.

As seen, the slope of ac curves changes drastically with the bias field increasing from 0 to 100 Oe. Fitting ac dependences to the Arrhenius equation the values of the activation energy E_a are obtained. For zero bias field the value of E_a equals 265 ± 5 K. The very low value of $\tau_0 = 7.8 \times 10^{-20}$ s is nonphysical. The values of E_a obtained for three nonzero values of bias field are much lower and all are equal to 84 ± 2 K. The values of τ_0 are $\sim 1.2 \times 10^{-9}$ s.

4.3. HF-ESR Study. HF-ESR measurements were undertaken to determine excitation gaps for *meta*-F and *ortho*-F compounds and thereby to get more insight into the relaxation character of these compounds. It should be noted, however, that in large magnetic fields, typical for HF-ESR, chains are effectively decoupled, thus only properties of individual chains are probed. The ESR spectra were measured at various frequencies and various temperatures.

4.3.1. meta-F Compound. Typical ESR spectra of the powder sample of *meta*-F compound measured at T = 4 K and various frequencies are shown in Figure 14a.

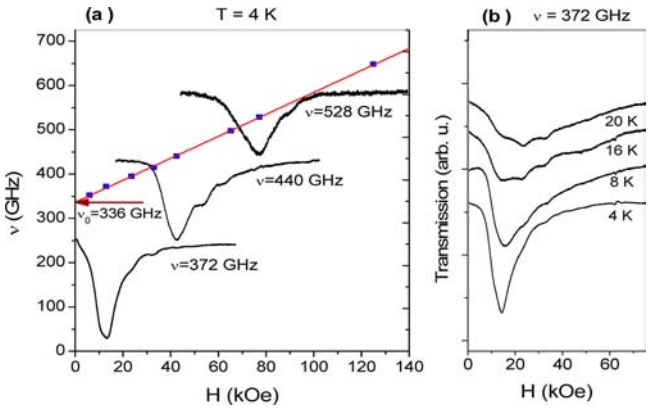

Figure 14. HF-ESR spectra of *meta*-F compound obtained at the temperature of 4 K for various frequencies (a) and at the frequency of 372 GHz for various temperatures (b). Panel a additionally contains frequency vs resonance magnetic field dependence (blue squares, experimental points; red line, linear fit).

The spectra comprise one intense transmission line, which narrows by decreasing excitation frequency ν. Variation of ν with field yields a linear shift of the resonance field H_{res}. This dependence is plotted in Figure 14a. The linear extrapolation to zero magnetic field gives the zero field splitting (gap) Δ_{ESR} = 336 GHz (16 K).

A representative set of the ESR spectra of the *meta*-F sample measured at constant frequency ν = 372 GHz and various temperatures is presented in Figure 14b. Here, a shift of the spectral weight to higher magnetic fields at higher temperatures takes place. Such a shift is a result of the thermal activation of the higher energy spin states with rising temperature and indicates a negative sign of the axial magnetic anisotropy of the chain.[39,40]

4.3.2. ortho-F Compound. ESR spectra measured for *ortho*-F are presented in Figure 15. Figure 15a shows spectra obtained at various frequencies at the temperature of 4.2 K. The small oscillations seen in the figure are extrinsic and due to some interference of the sample cell. Except for that, two characteristic features are seen. The first of them is the line width broadening at decreased resonance field. This is often caused by anisotropy in the plane normal to the principal axis of D; here, however, this anisotropy is lower than for the *meta*-F compound (see crystallographic data), which does not show the broadening but narrowing effect. The second feature is a small splitting of the line, which is well seen in Figure 15 at the lowest temperature of 4.2 K. Figure 15b shows the spectra at a constant frequency of 357 GHz obtained for various temperatures. Here it is seen that the line becomes broader and disappears with increasing temperature and no clear absorption is

dx.doi.org/10.1021/ic3014927 | Inorg. Chem. 2012, 51, 9983−9994

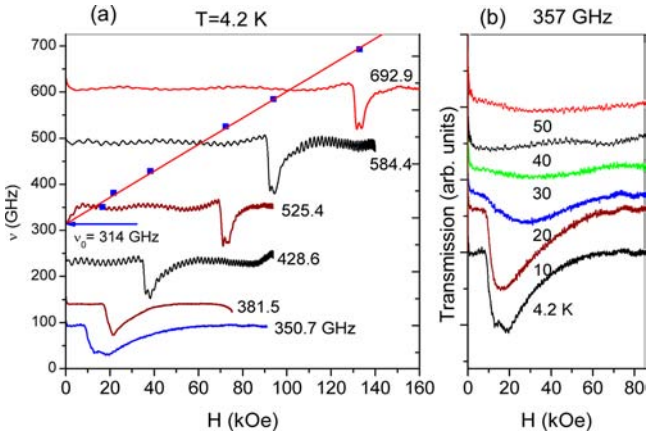

Figure 15. HF-ESR spectra of *ortho*-F compound obtained at various frequencies at the temperature of 4.2 K (a) and at the frequency 357 GHz for various temperatures (b). Panel a additionally contains frequency vs resonance magnetic field dependence (blue squares, experimental points; red line, linear fit).

found at 50 K. The observed splitting of the line seems to be connected with the crystallographic structure in which the $[TCNE]^-$ group has two orientations with the probability ratio 4:1.[5] The linear extrapolation of the mode gives the zero field splitting of Δ_{ESR} = 314 ± 3 GHz or 15.0 K (average of two peaks), see Figure 15a.

5. DISCUSSION

Both chain compounds investigated in this work show slow relaxations. While the *meta*-F compound shows the transition to the glassy ferromagnetic state at T_c = 10 K and in the applied dc field the SCM behavior, the *ortho*-F compound is a typical SCM. The question arises, what is the reason for such a difference, the more that intrachain magnetic interaction in *meta*-F is much weaker than in *ortho*-F. In response we would like to note that, first, in *ortho*-F we had finite chains in both ac and dc regimes,[9] while in *meta*-F the chains might be infinite in the ac regime. Second, *meta*-F has a structure with two different chain directions for which stronger dipolar superspin interactions may develop.[41]

The glassy character of *meta*-F compound at zero dc field was revealed by time dependent dc magnetization measurements and confirmed by ac susceptibility measurements. Both methods demonstrated a broad relaxation time distribution. For [MnTPP]-[TCNE]·2(1,3-$C_6H_4Cl_2$), belonging to the same compound family, Etzkorn et al. proposed the fractal cluster glass model, in which slow relaxations near the glass transition T_g are due to magnetic viscosity caused by interchain interactions.[12] We repeated the scaling analysis of Etzkorn et al., which led them to the above-mentioned conclusion. This analysis was based on the critical slowing down power law. However, we found results of scaling analysis not convincing because scaling with other laws gave also good overlapping of corresponding curves. In our opinion we are dealing with a true phase transition. Inclinations of spins due to different easy magnetic directions may favor ferromagnetic dipolar interchain interactions being responsible for 3D magnetic ordering.

The glassiness observed may be explained as due to 3D-domain wall pinning resulting from interchain interactions and lattice defects.[11,34] The domains that form consist of coupled spins belonging to some number of adjacent chains. Domain relaxations contribute to one of the two observed relaxation time distributions, namely, to the longer time distribution. In the bias dc magnetic field the glassy character is lost when with increasing field the domain walls are swept away. The only existing relaxations are now those of SCM having the narrow time distribution.

In order to get insight into the spin dynamics of *meta*-F it is helpful to inspect the activation energies obtained from measurements. In general, the activation time for magnetization reversal can be described by three activation energies, E_A, Δ_ξ and Δ_A, which obey the equation

$$E_A = 2\Delta_\xi + \Delta_A \tag{6}$$

assuming that chains are infinite or

$$E_A = \Delta_\xi + \Delta_A \tag{7}$$

when chains are finite. Chains may be treated as finite when they are shorter than their correlation length, what may happen with decreasing temperature. These equations are well proved for Ising chains, where Δ_A is the activation energy of a single anisotropic spin inside a narrow domain wall, where it sees no local field.[37] In the anisotropic Heisenberg model this value is still not well-defined. It should be related to anisotropy energy of a broad 1D domain wall.

If we assume that for *meta*-F at higher temperatures, in the ac regime, eq 6 is valid, then we have E_A = 84 K, Δ_ξ = 2 × 25 K, so Δ_A = 34 K. At lower temperatures, in the dc regime when eq 7 is valid, then we have E_A = 64 K, Δ_ξ =25 K, so Δ_A = 39 K. For *ortho*-F we had the finite chains only, then E_A = 117 K, Δ_ξ = 60 K[9] and Δ_A = 57 K. Assuming that the observed phase transition in *meta*-F is soliton induced, all π kinks should be paired below T_c. It would mean that for *meta*-F Δ_ξ values near T_c (in the ac regime) should be taken with the factor 2.

The *meta*- and *ortho*-F compounds differ much with the exchange parameter J, which equals −100 K for *meta*-F and −217 K for *ortho*-F. Treating the ferrimagnetic chain as a ferromagnetic chain composed of identical units with the effective spin S_{ef} = 3/2 one can estimate the exchange constant J_{ef} of such a chain. We used the following relation (eq 8) derived from the isotropic Hamiltonian (eq 9) of the ferromagnetic Heisenberg chain:[42]

$$\chi_{mol} = N_A g^2 \mu_B{}^2 \frac{2}{3J_{ef}} \left(\frac{J_{ef} S^2}{k_B T} \right)^2 \tag{8}$$

$$\mathcal{H} = -J_{ef} \sum_{\langle i,j \rangle} S_i S_j \tag{9}$$

The $1/T^2$ behavior of eq 8 is right at low temperatures only. In fact, the Seiden model shows also $1/T^2$ behavior at low temperatures, but we use eq 8 because it was derived from the simple Hamiltonian (eq 9) for which many other useful formulas were derived. In Figure 16 molar susceptibilities of *meta*- and *ortho*-F compounds as a function of $1/T^2$ are presented. The interval of fitting was chosen so that its higher limit is below T_{min} and the lower limit is the same as used by fitting of the Seiden model. The following values of J_{ef} were obtained: 28 ± 4 K for *meta*-F and 51 ± 4 K for *ortho*-F, assuming g factor equal to 2. Using these values and assuming that the single ion anisotropy is comparable for both compounds, we see that for both compounds $|D/J_{ef}| \ll 1$.

Being beyond the Ising limit $|D/J_{ef}| = 4/3$[37] both compounds cannot be SCM according to the original Glauber model.[43,44]

dx.doi.org/10.1021/ic3014927 | *Inorg. Chem.* 2012, 51, 9983−9994

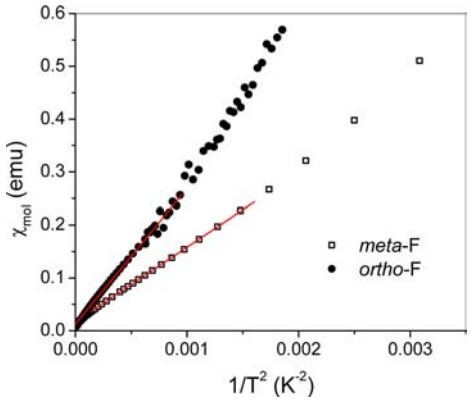

Figure 16. Molar susceptibility as a function of $1/T^2$ plotted for *meta*-F and *ortho*-F compounds. Solid lines are linear fits.

However, it was shown that SCM behavior also for $|D/J| \ll 4/3$ is possible.[37,45] In the case of extremely small anisotropy, Δ_ξ can be independently estimated using a simple expression:[46]

$$\Delta_\xi \approx 2S_{\text{eff}}{}^2 |2J_{\text{ef}} \cdot D|^{1/2} \quad (10)$$

Taking the earlier estimated values of D equal to 2.1 and 3.0 K this gives $\Delta_\xi \approx 48.8$ and $\Delta_\xi \approx 78.7$ K for *meta*- and *ortho*-F respectively. Although J_{ef} is much lower than the real J, the values of Δ_ξ obtained are considerably greater than Δ_ξ values found from measurements. In Table 3 Δ_ξ and other activation energies obtained are given for comparison. In addition, literature values for the Ising system $[Mn_2(saltmen)_2Ni(pao)_2(py)_2](ClO_4)_2$ (abbreviated $[Mn^{III}{}_2Ni]$)[37,44,47] and anisotropic Heisenberg system $[Mn(5\text{-TMAMsaltmen})(TCNQ)](ClO_4)_2$ (abbreviated Mn^{III}-TCNQ) are enclosed,[45] where saltmen = *N*,*N*′-(1,1,2,2-tetramethylethylene) bis(salicylideneiminate), pao = pyridine-2-aldoximate, py = pyridine, 5-TMAMsaltmen = *N*,*N*′-1,1,2,2-tetramethylethylene bis(5-trimethylammoniomethylsalicylideneiminate, TCNQ = 7,7,8,8-tetracyano-*p*-quinodimethane.

Table 3. Comparison of Activation Energies Obtained from Ac/Dc Susceptibility and HF-ESR for *meta*-F and Selected Single Chain Magnets

compd syst	E_A (K)	$n \times \Delta_\xi$ (K)[a]	Δ_A (K)[a]	K_A (K)[b]	Δ_{ESR} (K)
meta-F anis. Heisenberg	84[c]	2 × 25	34	8.5	16.1
	64[d]	1 × 25	39		
ortho-F[9] anis. Heisenberg	117[c,d]	1 × 60	57	11.8	15.0
$[Mn^{III}{}_2Ni]$[37,44,47] Ising	74[c]	2 × 28	18	22.1	15.4
	55[d]	1 × 28	27		
Mn^{III}-TCNQ[45] anis. Heisenberg	94.1[c]	2 × 26.5	41.1	9.8	
	67.7[d]	1 × 26.5	41.2		

[a] $\Delta_A = E_A - n \times \Delta_\xi$; for infinite chains the factor n equals 2, otherwise it equals 1. [b] K_A: anisotropy energy obtained from saturation magnetization and eq 3. [c] Ac data. [d] Dc data.

The situation is the simplest and well established for $[Mn^{III}{}_2Ni]$. Because $[Mn^{III}{}_2Ni]$ is a SCM system with $|D/J| > 4/3$, the considered spin clusters (1D domains) have extremely narrow walls of the one spin width. In such a case the activation energy Δ_A (for spin reversal in the wall) should be equal to the single ion anisotropy energy DS^2. Looking in Table 3, in fact, we see rather good agreement of the average Δ_A value, obtained from two temperature regimes (with finite and infinite chains, respectively), with K_A value obtained for $[Mn^{III}{}_2Ni]$ compound from the saturation magnetization.[37] It is also worth noting a good fulfillment of eq 6 and 7 for the Heisenberg system Mn^{III}-TCNQ, however, the Δ_A value in this case is much greater than the K_A value.

Oshima et al. performed HF-ESR study of $[Mn^{III}{}_2Ni]$ single chain magnet[47] and determined the value of the excitation gap at T = 1.5 K. It equals 321 GHz (15.4 K). It is lower than the K_A value for this compound and is near the gap values of our more strongly coupled systems. Because in the frequency-field diagram no series of lines with multiple value of $g = 2$ appeared, the authors concluded that the observed mode is neither spin cluster excitation nor spin cluster resonance. This mode was attributed to the spin wave excitation obeying the ESR selection rule $\Delta S_z = \pm 1$. This conclusion was supported by theoretical analysis, which proved that spin wave excitation is lower in energy than spin cluster excitation if the single ion zero field splitting parameter $|D_{Mn}|$ is lower than 5.7 K. However, by increasing the $|D_{Mn}|$ value, spin wave excitation becomes greater in energy. This theoretical result of Oshima et al. is in agreement with an older paper of Johnson and Bonner,[48] where a linear ferromagnet with spin 1/2 in a small magnetic field was analytically treated in the whole anisotropy range between Ising and Heisenberg models and it was shown that for anisotropy lower than some specific value the dominant excitations are spin waves. For anisotropy greater than this specific value the dominant excitations are bound spin wave complexes.

The excitation gaps obtained from HF-ESR study for *meta*-F and *ortho*-F are comparable, equal to ∼16 K. This value is greater than the anisotropy energies K_A per molecule estimated from magnetization measurements 8.5 and 11.8 K for *meta*-F and *ortho*-F, respectively. However, it is much lower than the anisotropy gap Δ_A obtained from magnetic ac/dc measurements. So large values of Δ_A follow from the fact that both *ortho*-F and *meta*-F are anisotropic Heisenberg systems, which have spin clusters with broad domain walls (solitons). Therefore many spins may be involved in the dynamics of walls and no wonder that the activation energy Δ_A of τ_0 is greater than DS^2 (see also Mn^{III}-TCNQ in Table 3).

Another reason that the Δ_{ESR} value is much lower than the Δ_A value obtained from ac/dc measurements is that selection rules of ESR can choose the lowest energy excitations. In fact, Johnson and Bonner[48] showed that the effective magnetic excitation gap for the low temperature susceptibility at small magnetic fields corresponds to the bound spin complexes in the whole anisotropy range.

For the time being, the question, why three different single chain magnet systems, *meta*-F, *ortho*-F and Mn_2Ni, have nearly the same value of the Δ_{ESR} gap, is still open. This value, however, seems to be close to the single ion anisotropy of Mn^{3+} ion.

6. SUMMARY

The compound Mn(III) tetra(*meta*-fluorophenyl)porphyrin-tetracyanoethenide (*meta*-F) was synthesized and its crystal structure was determined. This structure is composed of ferrimagnetic chains. There are two chain directions, which correspond to two magnetic easy axis directions. The compound was studied by magnetic measurements and, together with the relative *ortho* compound, by HF-ESR. Magnetic properties of both compounds were compared. While the *ortho*-F compound is the single chain magnet, the compound *meta*-F shows a glassy ferromagnetic transition at 10 K. In applied dc magnetic field

dx.doi.org/10.1021/ic3014927 | Inorg. Chem. 2012, 51, 9983−9994

the domain walls, responsible for glassy behavior, are swept away, so magnetic relaxations acquire a narrow distribution of relaxation times and look as relaxations of a single chain magnet. Activation energies for soliton spin reversals and spin wave excitations were determined using ac susceptibility and HF-ESR techniques, respectively. It was concluded that *meta*-F and *ortho*-F compounds are Heisenberg systems with anisotropy, for which soliton excitations are higher in energy than spin wave excitations.

■ ASSOCIATED CONTENT

Supporting Information

Crystallographic data in CIF format. This material is available free of charge via the Internet at http://pubs.acs.org.

■ AUTHOR INFORMATION

Corresponding Author

*E-mail: z.tomkowicz@uj.edu.pl; haase@chemie.tu-darmstadt.de.

Notes

The authors declare no competing financial interest.

¶On leave from Bio-Organic Division, Bhabha Atomic Research Centre, Trombay, Mumbai-400 085, India.

■ ACKNOWLEDGMENTS

W.H. thanks the Internationales Büro des BMBF for supporting the bilateral German-Indian cooperation project IND 02/007 and the Deutsche Forschungsgemeinschaft DFG for the support via the project HA782/85. Z.T. thanks grant of Ministry of Science and Higher Education, Poland, Nr. N N202 103238. H.N. acknowledges the support by Coordination Program in Grant-in-Aid for Scientific Research on Innovative Areas by MEXT Japan. The work in Dresden was supported by the DFG through project FOR 1154 "Towards molecular spintronics".

■ REFERENCES

(1) Caneschi, A.; Gatteschi, D.; Lalioti, N.; Sangregorio, C.; Sessoli, R.; Venturi, G.; Vindigni, A.; Rettori, A.; Pini, M. G.; Novak, M. A. *Angew. Chem.* **2001**, *113*, 1810.

(2) Brandon, E. J.; Rittenberg, D. K.; Arif, A. M.; Miller, J. S. *Inorg. Chem.* **1998**, *37*, 3376.

(3) Fardis, M.; Diamantopoulos, G.; Papavassiliou, G.; Pokhodnya, K.; Miller, J. S.; Rittenberg, D. K.; Christides, C. *Phys. Rev.* **2002**, *B 66*, 064422.

(4) Rittenberg, D. K.; Miller, J. S. *Inorg. Chem.* **1999**, *38*, 4838−4848.

(5) Brandon, E. J.; Arif, A. M.; Burkhart, B. M.; Miller, J. S. *Inorg. Chem.* **1998**, *37*, 2792.

(6) Mascarenhas, F.; Falk, K.; Klavins, P.; Schilling, J. S.; Tomkowicz, Z.; Haase, W. *J. Magn. Magn. Mater.* **2001**, *231*, 172.

(7) Bałanda, M.; Falk, K.; Griesar, K.; Tomkowicz, Z.; Haase, W. *J. Magn. Magn. Mater.* **1999**, *205*, 14 −26.

(8) Griesar, K.; Athanassopoulou, M. A.; Soto Bustamante, E. A.; Tomkowicz, Z.; Zaleski, A. J.; Haase, W. *Adv. Mater.* **1997**, *9*, 45.

(9) Bałanda, M.; Rams, M.; Nayak, S. K.; Tomkowicz, Z.; Haase, W.; Tomala, K.; Yakhmi, J. V. *Phys. Rev.* **2006**, *B 74*, 224421.

(10) Pikin, S. A.; Tomkowicz, Z.; Pikina, E. S.; Haase, W. *JETP Lett.* **2007**, *85*, 639−643. Pikin, S. A.; Tomkowicz, Z.; Pikina, E. S.; Haase, W. *Ferroelectrics* **2007**, *361*, 1−12.

(11) Ishii, N.; Okamura, Y.; Chiba, S.; Nogami, T.; Ishida, T. *J. Am. Chem. Soc.* **2008**, *130*, 24.

(12) Etzkorn, S. J.; Hibbs, W.; Miller, J. S.; Epstein, A. J. *Phys. Rev. Lett.* **2002**, *89*, 207201.

(13) Pini, M. G.; Rettori, A.; Bogani, L.; Lascialfari, A.; Mariani, M.; Caneshi, A.; Sessoli, R. *Phys. Rev.* **2011**, *B 84*, 04444.

(14) Bogani, L.; Caneshi, A.; Fedi, M.; Gatteschi, D.; Massi, M.; Novak, M. A.; Pini, M. G.; Rettori, A.; Sessoli, R.; Vindigni, A. *Phys. Rev. Lett.* **2004**, *92*, 207204.

(15) Coulon, C.; Clérac, R.; Wernsdorfer, W.; Colin, T.; Miyasaka, H. *Phys. Rev. Lett.* **2009**, *102*, 167204.

(16) Miyasaka, H.; Takayama, K.; Saitoh, A.; Furukawa, S.; Yamashita, M.; Clérac, M. *Chem.—Eur. J.* **2010**, *16*, 3656−3662.

(17) Ishida, T.; Okamura, Y.; Watanabe, I. *Inorg. Chem.* **2009**, *48*, 7012.

(18) Izyumov, Yu.A.; Chernoplekov, N. A. *Neutron Spectroscopy*; Plenum Pub. Corp.: New York, 1994.

(19) Elmassalami, M.; de Jongh, L. J. *Physica* **1989**, *B 154*, 254.

(20) Hołyst, J. A.; Sukiennicki, A. *Phys. Rev.* **1988**, *B 38*, 6975. Hołyst, J. A.; Sukiennicki, A. *Phys. Rev.* **1983**, *B 28*, 4062.

(21) Morgunow, R.; Kirman, M. V.; Inoue, K.; Tanimoto, Y.; Koshine, J.; Ovchinnikov, A. S.; Kazakova, O. *Phys. Rev.* **2008**, *B77*, 184419.

(22) Krzystek, J.; Telser, J.; Pardi, L. A.; Goldberg, D. P.; Hoffman, B. M.; Brunel, L.-C. *Inorg. Chem.* **1999**, *38*, 6121−6129.

(23) Adler, A. D.; Longo, F. R.; Finarelli, J. D.; Goldmacher, J.; Assour, J.; Korsakoff, L. *J. Org. Chem.* **1967**, *32*, 476.

(24) Jones, R. D.; Summerville, D. A.; Basolo, F. *J. Am. Chem. Soc.* **1978**, *100*, 4416−4424.

(25) Summerville, D. A.; Cape, T. W.; Johnson, E. D.; Basolo, F. *Inorg. Chem.* **1978**, *17*, 3297−3300.

(26) Golze, C.; Alfonsov, A.; Klingeler, R.; Büchner, B.; Kataev, V.; Mennerich, C.; Klauss, H.- H.; Goiran, M.; Broto, J.-M.; Rakoto, H.; Demeshko, S.; Leibeling, G.; Meyer, F. *Phys. Rev.* **2006**, *B 73*, 224403.

(27) Nojiri, H.; Ajiro, Y.; Asano, T.; Boucher, J.-P. *New J. Phys.* **2006**, *8*, 218.

(28) Brandon, E. J.; Arif, A. M.; Burkhart, B. M.; Miller, J. S. *Inorg. Chem.* **1998**, *37*, 2792−2798.

(29) Seiden, J. *J. Phys. (Paris) Lett.* **1983**, *44*, L947.

(30) Rittenberg, D. K.; Miller, J. S. *Inorg. Chem.* **1999**, *38*, 4838−4848. Brandin, E. J.; Kollmar, C.; Miller, J. S. *J. Am. Chem. Soc.* **1998**, *120*, 1822−1826. Ribas-Arino, J.; Novoa, J. J.; Miller, J. S. *J. Mater. Chem.* **2006**, *16*, 2600−2611. Her, J.-H.; Stephens, P. W.; Bagnato, J. D.; Miller, J. S. *J. Phys. Chem. C* **2010**, *114*, 20614−20620.

(31) Nakamura, K.; Sasada, T. *Solid State Commun.* **1977**, *21*, 891.

(32) Etzkorn, S. J.; Hibbs, W.; Miller, J. S.; Epstein, A. J. *Phys. Rev.* **2004**, *B 70*, 134419.

(33) The justification of this procedure in the case of the unidirectional anisotropy was given by Miyasaka, H.; Takayama, K.; Saitoh, A.; Furukawa, S.; Yamashita, M.; Clérac, R. *Chem.—Eur. J.* **2010**, *16*, 3656−3662. See also Miyasaka, H.; Saitoh, A.; Yamashita, M.; Clérac, R. *Dalton Trans.* **2008**, 2422−2427.

(34) Sampaio, L. C.; da Cunha, S. F. *J. Magn. Magn. Mater.* **1990**, *88*, 151.

(35) Mydosh, J. A. *Spin Glasses: An Experimental Introduction*; Taylor & Francis: London, 1993.

(36) Bałanda, M.; Tomkowicz, Z.; Haase, W.; Rams, M. *J. Phys.: Conf. Ser.* **2011**, *303*, 012036.

(37) Miyasaka, H.; Julve, M.; Yamashita, M.; Clerac, R. *Inorg. Chem.* **2009**, *48*, 3420−3437.

(38) Kajiwara, T.; Nakano, M.; Kaneko, Y.; Takaishi, S.; Ito, T.; Yamashita, M.; Igashira- Kamiyama, A.; Nojiri, H.; Ono, Y.; Kojima, N. *J. Am. Chem. Soc.* **2005**, *127*, 10150−10151.

(39) Kahn, O., *Molecular Magnetism*; Wiley-VCH: Weinheim, 1993.

(40) Krupskaya, Y.; Alfonsov, A.; Parameswaran, A.; Kataev, V.; Klingeler, R.; Steinfeld, G.; Beyer, N.; Gressenbuch, M.; Kersting, B.; Büchner, B. *ChemPhysChem* **2010**, *11*, 1961−1970.

(41) Ostrovsky, S.; Haase, W.; Drillon, M.; Panissod, P. *Phys. Rev.* **2001**, *B 64*, 134418. Wynn, C. M.; Gîrtu, M. A.; Brinckerhoff, W. B.; Sugiura, K.-I.; Miller, J. S.; Epstein, A. J. *Chem. Mater.* **1997**, *9*, 2156−2163.

(42) Suzuki, F.; Shibata, N.; Ishii, C. *J. Phys. Soc. Jpn.* **1994**, *63*, 1539.

(43) Glauber, R. J. *J. Math. Phys.* **1963**, *4*, 294.

(44) Coulon, C.; Clérac, R.; Lecren, L.; Wernsdorfer, W.; Miyasaka, H. *Phys. Rev.* **2004**, *B 69*, 132408.

(45) Miyasaka, H.; Madanbashi, T.; Sugimoto, K.; Nakazawa, Y.; Wernsdorfer, W.; Sugiura, K.; Yamashita, M.; Coulon, C.; Clérac, R. *Chem.—Eur. J.* **2006**, *12*, 7028.
(46) ElMassalami, M.; Smit, H. H. A.; de Grot, H. J. M.; Thiel, R. C.; de Jongh, L. J. In *Magnetic Excitations and Fluctuations II*, Proceedings of an International Workshop; Balucani, U., Lovesey, S. W., Rasetti, M. G., Tognetti, V., Eds.; Turin, Italy, May 25−30, 1987; Springer Proceedings in Physics, Vol. *23*; Springer-Verlag: Berlin, 1987; p 178.
(47) Oshima, Y.; Nojiri, H.; Asakura, K.; Sakai, T.; Yamashita, M.; Miyasaka, H. *Phys. Rev.* **2006**, *B 73*, 214435.
(48) Johnson, J. D.; Bonner, J. C. *Phys. Rev.* **1980**, *B 22*, 251.